Poly(isosorbide carbonate): A 'green' char forming agent in polybutylene succinate intumescent formulation

Chi Hu, Serge Bourbigot, Thierry Delaunay, Marion Collinet, Sophie Marcille, Gaelle Fontaine

Contents lists available at ScienceDirect

Composites Part B

journal homepage: http://ees.elsevier.com

Poly(isosorbide carbonate): A 'green' char forming agent in polybutylene succinate intumescent formulation

Chi Hu [a,b,c], Serge Bourbigot [a], Thierry Delaunay [c], Marion Collinet [c], Sophie Marcille [d], Gaëlle Fontaine [a,*]

[a] Univ.Lille, ENSCL, UMR 8207, UMET, Unité Matériaux et Transformations, F59000, Lille, France
[b] China Academy of Engineering Physics, Institute of Chemical Materials, MianYang, China
[c] IFMAS, 60 Avenue Du Halley, 59650, Villeneuve-d'Ascq, France
[d] Roquette, Rue de La Haute Loge, 62136, Lestrem, France

ABSTRACT

A new flame retardant (FR) intumescent system for polybutylene succinate (PBS) was developed using poly(isosorbide carbonate) (PIC), a bio-based polymer, as a 'green' char forming agent. The use of this charring agent in PBS/ammonium polyphosphate (APP) permits to obtain better efficiency than PBS/APP alone for mass loss cone calorimetry (MLC) test: pHRR was decreased by 24% vs 19%, THR was decreased by 48% vs 25% and the yield of residue was increased to 44% vs 23% respectively. According to the temperature measured by thermocouples embedded in the sample, the char formed for PBS/PIC/APP showed a better heat barrier effect than that of PBS/APP: under the char, the temperature and the heating rate of PBS/PIC/APP is significantly lower than those of PBS/APP. Obvious differences of the chemical composition and the morphology of the chars highlight that the good results obtained for PBS/PIC/APP were governed by a glass type char formed during the MLC test.

1. Introduction

Bio-based polymers had great development during the last decades due for example to environmental concern caused by the petroleum-based polymers. Among these bio-based polymers, polybutylene succinate (PBS) has been widely used for short term applications i.e. packaging, agriculture, medical articles due to its bio-degradability and good mechanical properties (close to polypropylene and polyethylene) [1]. Furthermore, composites of PBS blending with inexpensive natural fibers provide better mechanical properties than neat PBS [2–5], which can be promisingly applied in some engineering field such as electric & electronic, construction and transportation. It is noteworthy that materials used in these fields of applications often need to be flame retarded according to legislation and industrial demands. However, like many organic thermoplastics, PBS is highly flammable, thus its application in these fields are limited. In this context, it is necessary to improve the flame retardancy of PBS.

Flame retardancy of PBS are often based on intumescent flame retardant system [6–13]. Most of these intumescent formulations are phosphorus and nitrogen based FRs. Use of synergists or novel char formers can significantly enhance the performance [9,10,12,13].

The use of polymer as char forming agent in an intumescent FR system has also been described in literature using polyamide (PA) [14,15] or polyurethane (PU) [16,17] where they were used in intumescent FR system. Since polyols such as pentaerythritol, mannitol and sorbitol are considered as a carbonization agent in intumescent FR system [18,19], Poly(isosorbide carbonate) (PIC) which is a polycarbonate derived from isosorbide (a saccharide derived from starch) may thus be potentially used as a char forming agent. Moreover, using PIC in PBS may promisingly provide double advantages: i) a 'green' formulation formed with two types of bio-based polymers; ii) an enhanced intumescent FR system by using a char forming agent. Therefore, in this paper, the fire performances of formulations containing PIC and ammonium polyphosphate (APP) is firstly investigated by mass loss cone calorimetry (MLC). The best ratio of PIC/APP was determined and used to deeply understand the effect of PIC in the formulation. Thus, its mass loss and the temperature evolution inside the char during the MLC test were investigated. The chemical composition of the char, thermal decomposition behavior and the char morphology are also presented. A mode of action of these intumescent FR systems (PBS/APP and PBS/PIC/APP) during the MLC test is proposed in the last part.

* Corresponding author.
E-mail address: gaelle.fontaine@ensc-lille.fr (G. Fontaine)

https://doi.org/10.1016/j.compositesb.2019.107675
Received 29 August 2019; Received in revised form 29 November 2019; Accepted 30 November 2019
Available online xxx
1359-8368/

2. Experimental

2.1. Materials

The polymer used is PBS bionolle™ 1001MD, which was supplied by Showa Denko (Japan). Poly (isosorbide carbonate) (PIC), DURABIO™ D7340 is based on isosorbide which is supplied by Mitsubishi Chemical (Japan). Ammonium polyphosphate (APP) Exolit® AP 422 was supplied by Clariant (Swiss).

2.2. Processing

PBS, PIC and APP are mixed in a DSM Xplore Micro15 twin-screw micro-extruder at 160 °C for 10 min with a rotating speed of screw of 50 rpm. Square shape samples (50 × 50 × 3 mm) for MLC tests are prepared by compression molding at 160 °C, 20 kN for 2 min, 40 kN for 6 min.

2.3. Fire test

The fire test used in the study is a Fire Testing Technology (FTT) mass loss calorimeter (MLC) device (ISO 13927, ASTM E906). The distance between the sample holder and the heat source was 25 mm. An external heat flux (35 kW/m^2) produced by a conical heater element is applied to the sample. The temperature of the gaseous combustion products is measured at the top of the chimney with a thermopile. The efficiency of the formed char acting as heat barrier was evaluated by thermocouples embedded in the plaques. The position of the thermocouples is presented in Fig. 1. The first thermocouple (T1) was placed under the plaques in order to measure the temperature of the bottom, whereas the second thermocouple was placed on the surface of the plaque through a drilled hole (T2) to measure the surface temperature of the plaque. It is noteworthy that T2 remains always 3 mm height above the bottom. Therefore, in the case of neat PBS, T2 measures the surface temperature of the material until the thermocouple is no longer embedded in the matter (after the ignition). In the case of PBS/APP and PBS/PIC/APP, T2 measures the surface temperature before the ignition and also after the ignition because of the formation of the intumescent char. T2 remains embedded in the char and heat gradient can be measured between T1 and T2. The measurement by thermocouples remains an error margin within ±30 °C.

2.4. Solid state NMR

^{13}C NMR measurements were done using a Bruker Avance spectrometer and a 4 mm probe, operating at 100.6 MHz (9.4 T) with magic angle spinning (MAS) (spinning frequency: 10 kHz). Tetramethylsilane was used as reference for 0 ppm.

^{31}P NMR measurements were performed on a Bruker Avance II spectrometer, operating at 161.9 MHz (9.4 T) and at a spinning rate of 12.5 kHz with magic angle spinning. Bruker probe heads equipped with 4 mm MAS assembly were used. Experiments have been carried out using cross polarization (CP) ^{1}H-^{31}P because of the long relaxation time of the phosphorus nuclei (10–500 s) with ^{1}H high power dipolar decoupling (HPDEC). H_3PO_4 in aqueous solution (85%) was used as reference for 0 ppm.

2.5. Thermal analysis

Thermogravimetric analysis (TGA) measurements were carried out on a Setaram TG92-16. Samples were contained in silica crucibles robed with gold sheet. They were grinded into powder using a cryo-grinder (500 μm filter) before the analysis. Fluid flow rate was set at 100 mL/min, air was chosen to evaluate the decomposition of the materials in thermo-oxidative conditions. A heating rate of 10 °C/min was used. When TGA was used to investigate the thermal behaviors of the used materials during the MLC test, the heating rates were set according to the temperature evaluation measured by the thermocouple 2 (T2) to mimic the same experiment condition in MLC test.

2.6. Morphology analysis of the char

The char morphology on a millimeter (mm) scale was measured by optical microscope and carried out on a Keyence - VHX-1000 digital microscope. Measurements were repeated ten times on randomly chosen parts of the char, to ensure representative values.

The char morphology on a micrometer (μm) scale was measured by scanning electron microscope (SEM) carried out on a Hitachi S4700 at 6 kV. All the samples were microtomed with a diamond knife on a Leica UltraCut microtome at cryogenic temperature (−120 °C) to obtain smooth surfaces. The distribution of the phosphorus in the char was measured by electron probe microanalysis (EPMA) (Cameca – SX 100). This measurement shares the same samples prepared for the SEM.

3. Results and discussion

3.1. Fire properties of PBS/PIC/APP formulations

The efficiency of PIC acting as char forming agent was evaluate by MLC test and it is presented in Fig. 2 and Table 1.The additives were incorporated at 30 *wt*% in PBS. When only 30 *wt*% of PIC was added to PBS, no improvement of the flame retardancy of PBS was observed. When 30 *wt*% of APP was added in PBS, pHRR is decreased by 19% and the THR is decreased by 25%. Different ratio of PIC/APP (3/1, 1/1, 1/3) was evaluated. The best result is obtained when the ratio of PIC/APP is at 1/3. With this ratio, pHRR is decreased by 24%, the THR is decreased by 48% and the char yield can reach 44%. Compared to the formulation without the carbonization agent, the formulation PBS/PIC/

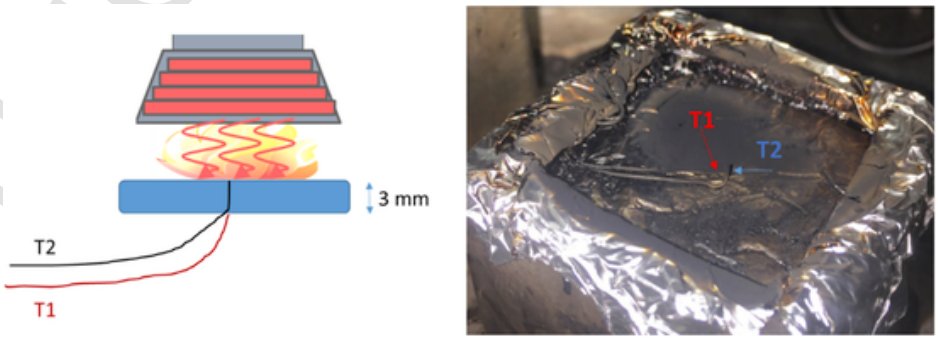

Fig. 1. Position of the thermocouples (left), in real situation (right).

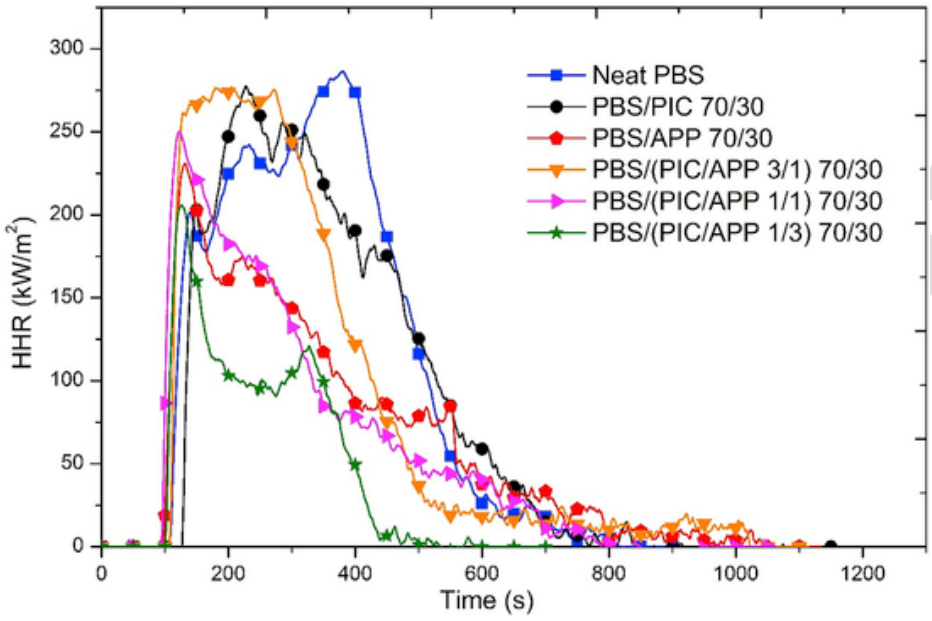

Fig. 2. MLC tests of PBS with PIC and APP (50 x 50 × 3 mm^3, 35 kW/m^2, 25 mm).

Table 1
Results of MLC tests of PBS with PIC and APP.

Ratio [*wt.*%]	pHRR [kW/m ^{2}]	THR [MJ/m ^{2}]	$t_{ignition}$ [s]	$t_{flameout}$ [s]	residue
Neat PBS	283	91	110	605	2%
PBS/PIC 70/30	275 (−2%)	88	126	767	1%
PBS/APP 70/30	231 (−19%)	67 (−25%)	99	712	23%
PBS/(PIC/APP 3/1) 70/30	277 (−2%)	84 (−8%)	110	490	9%
PBS/(PIC/APP 1/1) 70/30	250 (−11%)	61 (−33%)	112	766	18%
PBS/(PIC/APP 1/3) 70/30	216 (−24%)	47 (−48%)	105	484	44%

APP exhibits an enhanced performance for the main parameters measured at MLC. The formation of the char in this formulation may be the key point of the successful results. The residual char of PBS/APP 70/30 had obvious cracks and holes on the surface (Fig. 3). Whereas the char of PBS/PIC/APP exhibits only small holes (Fig. 3). Investigations for mechanism elucidation were performed on PBS, PBS/APP and PBS/PIC/APP (1/3) formulations and are presented hereafter.

3.2. *Investigation of the mass loss and temperature evolution during MLC test*

The MLC results along with the mass loss are presented in Fig. 4 a) Fig. 4 b). From the beginning of the experiment to the ignition (110 s for neat PBS, 99 s for PBS/APP and 100 s for PBS/PIC/APP), the materials softened and melted without significant mass loss. From the ignition to 200 s, the char can be visually observed in the formulation of PBS/APP and PBS/PIC/APP. Neat PBS had 6% of mass loss, and it started to degrade with a high mass loss rate (0.25%/s) until the matter had almost totally burned out. However, PBS/APP and PBS/PIC/APP kept a low mass loss rate during the formation of the char, corresponding to only 1% of mass loss. From 200 s to 330 s, visual observation indicates that the chars of PBS/APP and PBS/PIC/APP kept a stable state (no cracking) at the beginning (200 s–270 s), then cracked a little (270 s–330 s) according to the MLC curve i.e. increase of the pHRR. The mass loss rate of PBS/APP starts to increase to 0.17%/s at 200 s, and PBS/PIC/APP reaches a similar mass loss rate at 230 s. After 300 s, PBS/APP kept the same mass loss rate (0.17%/s) up to 600 s, but the

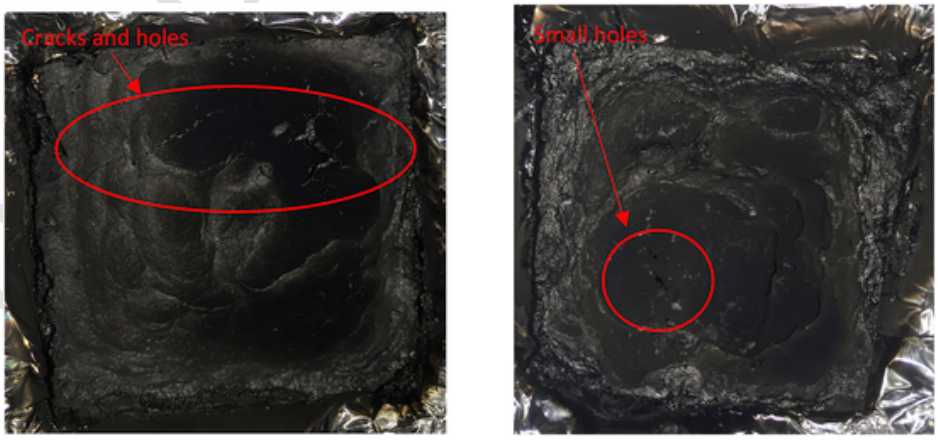

Fig. 3. MLC residual char of PBS/APP 70/30 (left) and PBS/(PIC/APP 1/3) 70/30 (right).

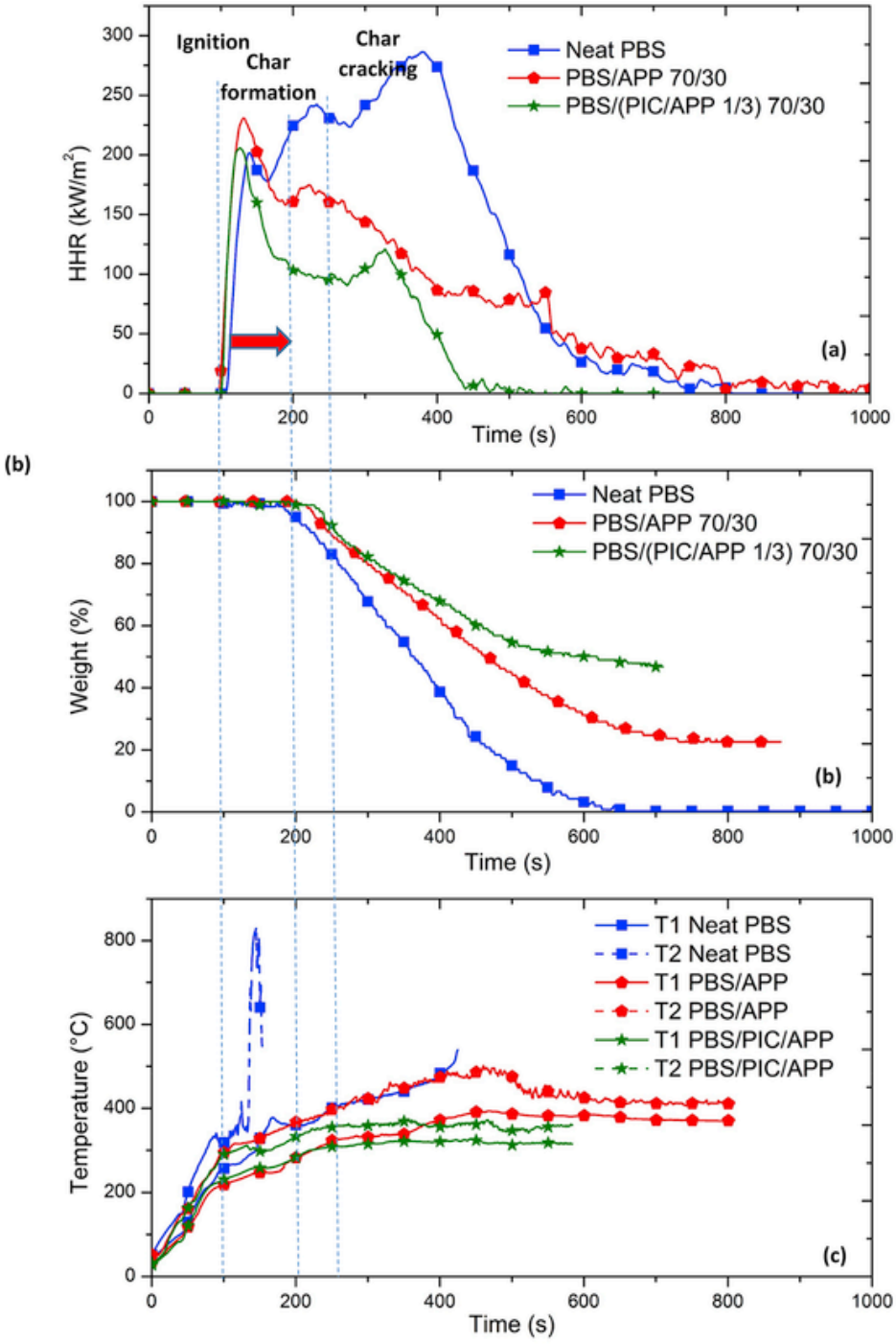

Fig. 4. a) MLC test of PBS, PBS/APP and PBS/PIC/APP, b) mass loss during the MLC test, c) temperature measured by the thermocouples (T1 – bottom; T2 – surface).

mass loss rate of PBS/PIC/APP decreased continuously to only 0.03%/s at 600 s. The final residue of neat PBS was almost 0%, that of PBS/APP was 23% and that of PBS/PIC/APP was 44%.

Temperatures profiles measured by thermocouples are presented in Fig. 4 c). It shows that before ignition, the surface of all three materials have similar heating rate (about 180 °C/min). At ignition the surface temperature (T2) of PBS (110 s), PBS/APP (99 s) and PBS/PIC/APP (100 s) is 330 °C, 296 °C and 291 °C respectively. The similar heating rate and surface temperature suggests that the incorporation of the additives does not modify significantly the thermo-physical properties of PBS. On the bottom of the plaques (T1), the temperature of PBS is 83 °C lower than that of the surface, while for PBS/APP and PBS/PIC/APP the temperatures are 72 °C and 69 °C lower than the surface temperatures respectively.

From the ignition (110 s) to 200 s, the heating rate of T1 for neat PBS is quite high and estimated at 80 °C/min, and the temperature of T1 increased continuously up to 465 °C until the thermocouple is no longer embedded in the matter (about 400 s). For PBS/APP, the char formation is visually observed between 100 s and 200 s. T1 and T2 curves of PBS/APP exhibit similar evolution and are parallel during this stage. The heating rate (measured via T1 or T2) is estimated at 40 °C/min (100 s–200 s) and is twice lower than that of neat PBS. For PBS/

PIC/APP, the char formation was also visually observed between 100 s and 200 s. During its formation, T1 of PBS/PIC/APP exhibits similar temperature of that of PBS/APP, but T2 is 20 °C lower than that of PBS/APP. It is noteworthy that the heating rate of T2 is about 24 °C/min and is significantly lower than that of PBS/APP. It can explain at least partially, why at 200 s the HRR of PBS/PIC/APP is 51 kW/m^2 lower than that of PBS/APP.

From 200 s to 330 s, T1 and T2 of PBS/APP measure the same heating rate (40 °C/min), and the bottom temperature (T1) of PBS/APP shows that a temperature gradient between T1 and T2 is more than 70 °C. Whereas for PBS/PIC/APP, T1 and T2 reach a stable plateau (steady state) after the formation of the char (200 s) until the end of the test (583 s, T2 - T1 = 45 °C).

After 330 s, T1 and T2 of PBS/APP increased up to 372 °C (485 s) and 471 °C (485 s) respectively. T1 and T2 of PBS/APP always increase from 100 s to 485 s even after the formation of the char. This indicates heat barrier of the char has low efficient. Afterward, T1 and T2 decrease and reach a steady state at 370 °C and 410 °C respectively. The temperature gradient between T1 and T2 at this steady state is only 40 °C. As for PBS/PIC/APP, the temperature gradient between T1 and T2 at the steady state is 45 °C. Moreover, these two plateaus observed with PBS/PIC/APP have always lower temperatures than those measured in the case of PBS/APP i.e. PBS/PIC/APP T1 equals 315 °C vs PBS/APP T1 equals 370 °C and PBS/PIC/APP T2 equals 360 °C vs PBS/APP T1 equals 410 °C.

These results evidence that the char of PBS/PIC/APP is more efficient than that of PBS/APP in term of heat barrier. Its relatively low heating rate under the char leads to a lower decomposition rate of the polymer, which can explain the low pHRR and THR. The formation of char is related to a series of chemical reactions and so, the investigation of the chemical composition of the char during MLC test would help understanding the mechanism of action of these two formulations. Therefore, the next part focuses on the nature of the char at different stage of the MLC test.

3.3. Investigation of the chemical composition of the char by solid state NMR

The chemical composition of the char at different MLC stage test was investigated using solid state NMR. The considered nuclei are ^{31}P and ^{13}C. The residual chars were collected at three different stages of the MLC test i.e. (i) at 120 s when the char started to form; (ii) at 250 s when the char is stabilized; (iii) at 420 s when the heat release rate decreased.

3.3.1. Characterization of ^{31}P NMR

The MAS ^{31}P spectra of PBS/APP 70/30 and PBS/(PIC/APP 1/3) 70/30 are presented in Fig. 5. It was found that during the solid state NMR experiment, the presence of phosphoric acid may cause explosion of the rotor during the rotation in the probe, which may cause severe damage to the probe (viscous phosphate trapped in the char creates a pressure on the rotor cap which is ejected). Thus, the chars were washed with water and dried under 90 °C for 24 h prior to be analyzed. Only two samples (PBS/APP stage 1 and PBS/APP stage 2) were analyzed without washing and thus can be compared with the samples after the washing (Fig. 5).

Before the MLC test, the MAS ^{31}P NMR of the un-burned PBS/APP and PBS/PIC/APP showed a doublet at −21.5 ppm and −22.5 ppm, which are assigned to P-O in the APP [20,21]. The same chemical shift of the phosphorus for neat APP is observed indicating that no chemical reaction of PBS or PIC occurred with APP during the processing (extrusion and compressing molding). At the stage 1 (120 s), for the PBS/APP and PBS/PIC/APP washed samples, a broad band centered at 0.5 ppm is observed. This band can be assigned to orthophosphate linked with aliphatic groups and/or orthophosphoric acid [14,20,21]. The shape and the width of the band indicates a disordered structure suggesting a glass-type behavior. At the stage 2 (250 s), for PBS/APP, besides the band at 0 ppm, a narrow sharp band was found at 2.3 ppm, which can be assigned to the P-O-C group (might be orthophosphate linked with ester groups) [22,23]. PBS/PIC/APP exhibits similar two bands at 0 ppm and 2.3 ppm, but the band at 0 ppm shows a flattened feature, which indicates that the orthophosphates may be less ordered than those of PBS/APP. At the stage 3 (420 s), for PBS/APP, the two bands at 0 ppm and 2.3 ppm are still observed but unlike the stage 2, the ratio between the band at 2.3 ppm and the band at 0 ppm changed from 1 : 1.2 (stage 2) to 1 : 3.9 (stage 3). For PBS/PIC/APP, the band at 0 ppm shows a more flattened feature. The final chars of these two formulations present only a broad band at 0 ppm suggesting a disordered structure like a glass-type structure.

Un-treated samples showed different behavior than washed ones in MAS ^{31}P spectra (Fig. 5). For un-treated char of PBS/APP at stage 1 and stage 2, three bands were presented at 0 ppm, −12.1 ppm and −25.3 ppm. Like the washed samples, the band at 0 ppm can be assigned to the orthophosphoric acid and/or orthophosphate groups linked to the aliphatic groups. Then the band at −12.1 ppm may possibly be assigned to the pyrophosphate groups and/or orthophosphate linked to the aromatic groups (di-phenylorthophosphate and tri-phenylorthophosphate) [21,24]. It was found that after washing, the band at −12.1 ppm disappeared, which reveals that only the free pyrophosphate groups were produced. To attribute the band at −25.3 ppm, the phosphates that contain a single PO_4 or multiple PO_4 linked with each others are noted as follows (Fig. 6): i) Q_0, phosphate that has a single PO_4, ii) Q_1, phosphate that contains one bridged oxygen, iii) Q_2, phosphate that has two bridged oxygen and iv) Q_3, phosphate that has a ramified structure which contains three bridged oxygen. Thus, the band at −25.3 ppm can be assigned to the phosphate in a Q_2 structure [25]. It is noteworthy that this band is broad which indicates the structure of these phosphates are disordered.

With the information provided above, the evolution of phosphorus in PBS/APP and PBS/PIC/APP during MLC test can be concluded. The decomposition of the matter formed Q_0 structure orthophosphates linked to aliphatic groups, Q_1 structure pyrophosphates that do not link with aromatic groups and Q_2 structure phosphates. Then the Q_1 structure orthophosphates that contained a P-O-C structure was formed. Specially, at this stage, the band of the orthophosphates linked with the aliphatic groups of PBS/PIC/APP is broader and more flattened than that of PBS/APP, which shows that the incorporation of PIC increased the disorder of the phosphate species. This disordered structure indicates the formation of a glass-type structure, which can be a reason that the PBS/PIC/APP has better performance than PBS/APP in MLC test [26]. Finally, only the orthophosphates that linked with the aliphatic groups are found in the final char.

3.3.2. Characterization of ^{13}C NMR

The magic angle spinning (MAS) ^{13}C spectra of PBS/APP 70/30 and PBS/(PIC/APP 1/3) 70/30 are presented in Fig. 7.

Before the fire test, neat PBS exhibit four bands at 25.6 ppm, 29.1 ppm, 64.3 ppm and 172.6 ppm. The band at 25.6 ppm is assigned to the -CH_2- in the butylene part that are not bounded to the oxygen. The band at 29.1 ppm is assigned to the -CH_2- of the succinate part. The band at 64.3 ppm is assigned to the -CH_2-O- of the butylene part, and the band at 172.4 ppm is assigned to the carbon of the carbonyl group [27,28]. When PBS was blended with APP and PIC, these four bands showed the same chemical shift as neat PBS, hence it confirms that there is no chemical interaction during the processing. Neat PIC presents an obvious band at 155.3 ppm which can be assigned to the carbonate group [29]. It presents also a broad band between 70 ppm

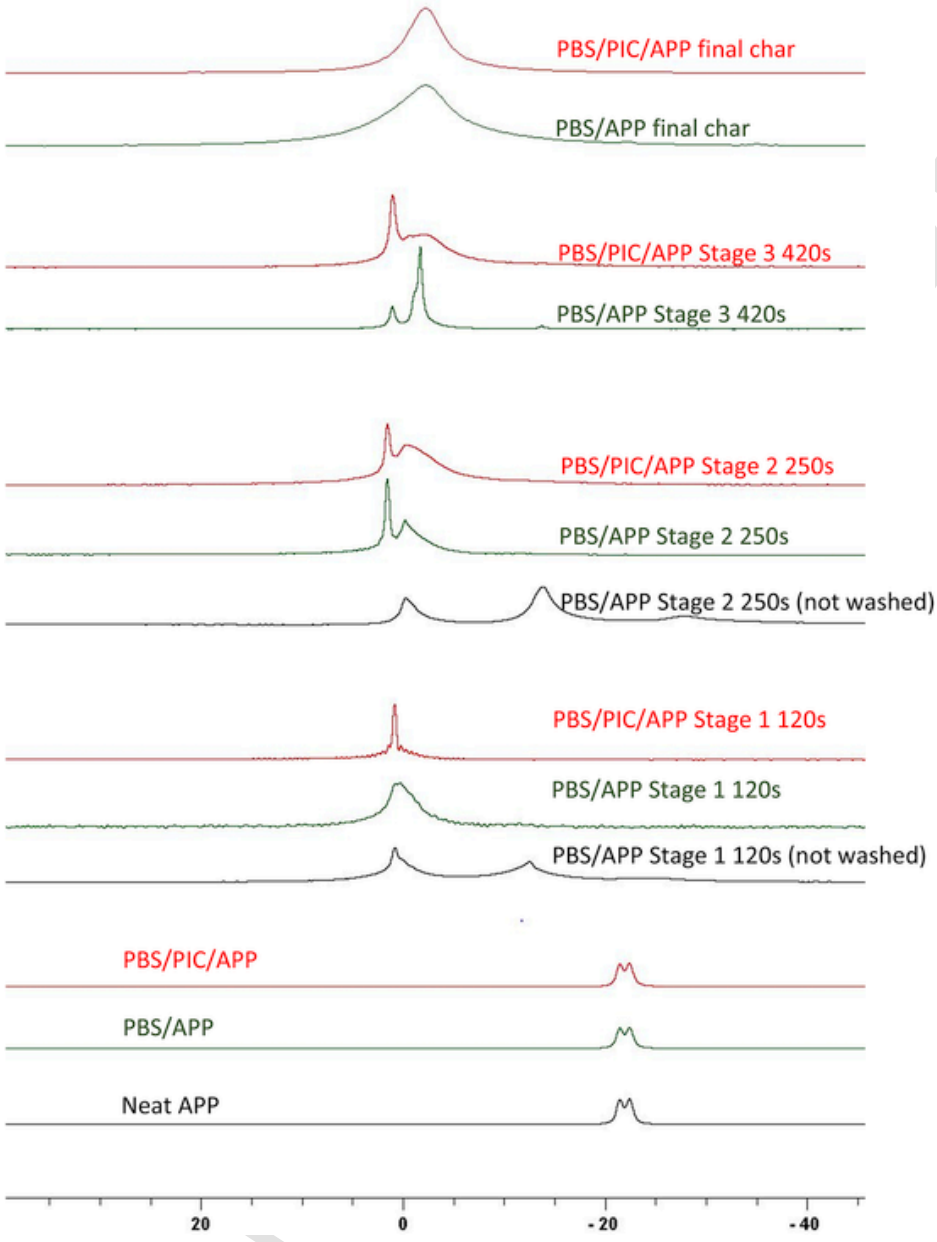

Fig. 5. Solid state NMR MAS ^{31}P spectra of PBS/APP and PBS/PIC/APP formulations collected at different stage of the MLC test.

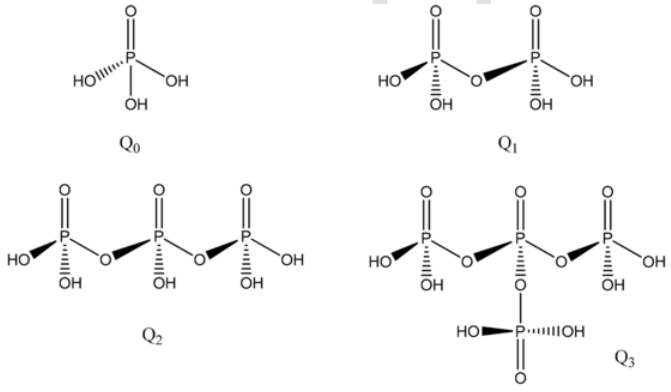

Fig. 6. Nomenclature of the different types of phosphate.

and 90 ppm which can be assigned to the carbon of the isosorbide group.

For the samples at 120 s, 250 s 420 s and the final char, there is a broad band at 130 ppm. It can be assigned to unsaturated carbon (C═C, aromatic and polyaromatic species) [30,31]. This band became more and more intense with the evolution of the time, which indicate that an aromatization occurring during the formation of the char. A broad band was also found at about 30 ppm which can be assigned to the aliphatic carbons [30,32]. For PBS/APP and PBS/PIC/APP, they showed similar ^{13}C NMR spectra, which indicates that the incorporation of PIC had no significant change on the chemical composition of the char.

3.4. Thermal stability analysis

To understand the decomposition behavior of the different formulations and the formation of residual char, thermal stability of PBS/APP

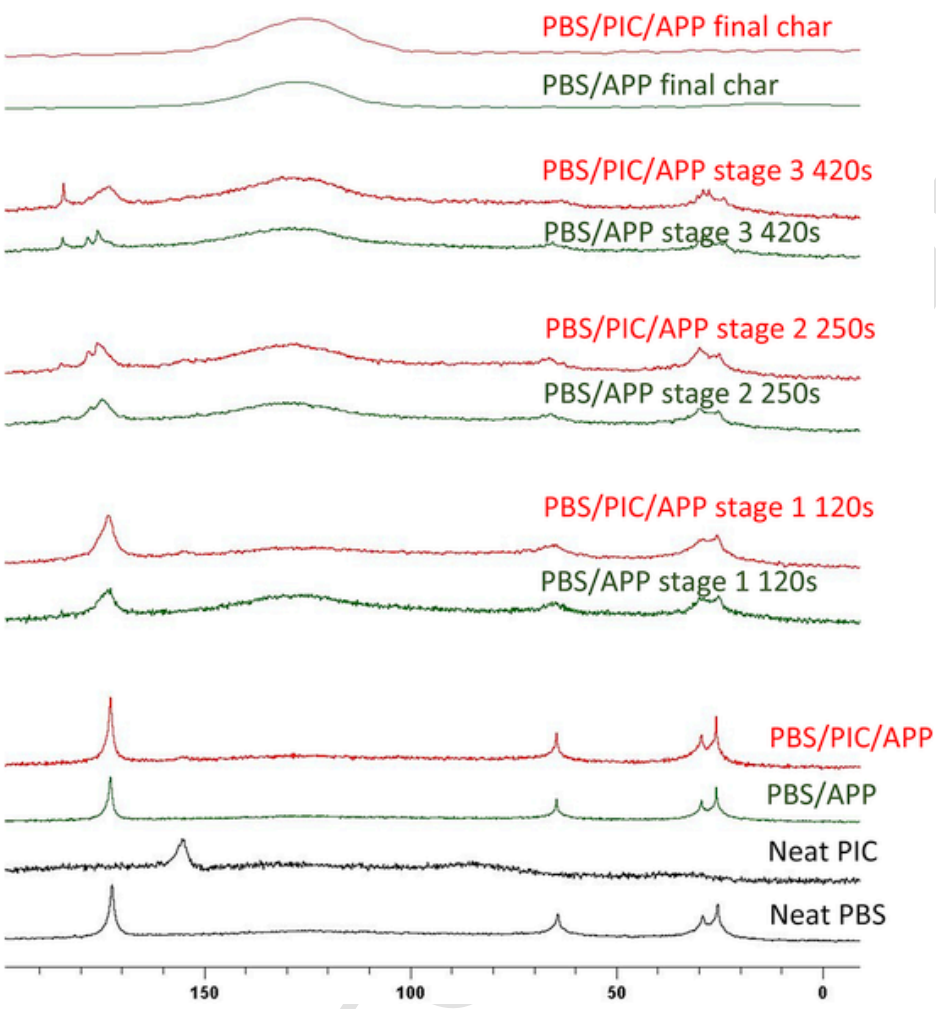

Fig. 7. Solid state NMR MAS ^{13}C spectra of PBS/APP and PBS/PIC/APP at different stage.

70/30 and PBS/(PIC/APP 1/3) 70/30 are analyzed under thermo-oxidative condition. In this part, 2% of mass loss (T2%) is considered as the starting of the degradation.

The thermal stability of neat PBS and the formulations with additives under thermo-oxidative conditions was investigated by TGA (Fig. 8). APP exhibits a two-step decomposition process. The first step ranges

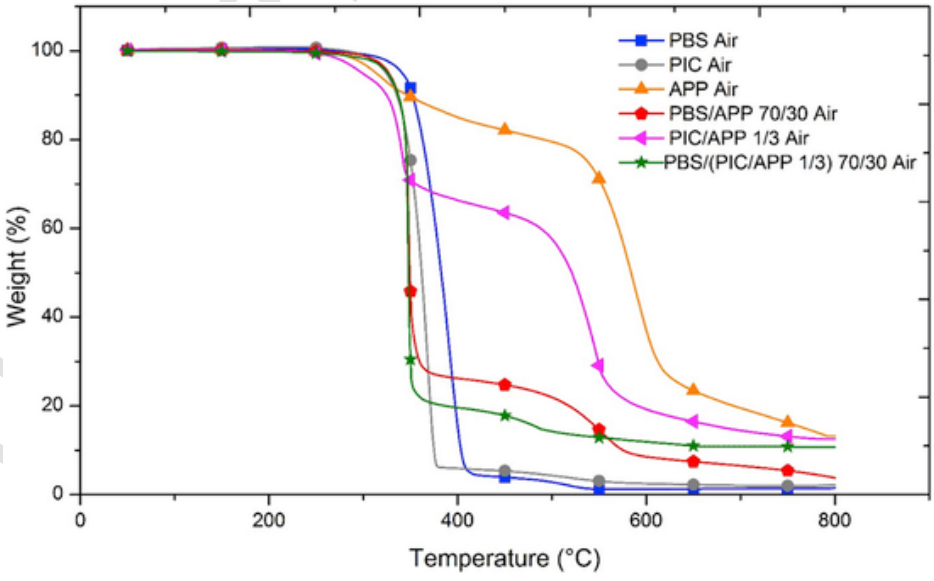

Fig. 8. Thermal degradation of PBS with the additives under thermo-oxidative condition (10 °C/min, Air).

from 250 °C to 450 °C with a mass loss of 18%, and this mass loss corresponds to the release of water and ammonia [33]. Meanwhile, a cross linked P-O-P structure formed by elimination of H_2O between P-OH groups, and these P-OH groups were released by the evolution of NH_3. The second step range from 450 °C to 650 °C with a mass loss of 59% can be assigned to the release of phosphoric acid [34,35]. It is noteworthy that the residue of APP has low stability at high temperature. The residue mass decreases continuously from 23.6% at 650 °C to 12.5% at 800 °C.

The decomposition of PBS involves two steps of process. The first step ranges from 323 °C to 417 °C with a mass loss of 94.3%. This step is attributed to depolymerization of the PBS, tetrahydrofuran and succinic anhydride are the main decomposition products [36]. The second step, from 417 °C to 520 °C, is the formation and the degradation of a transient char. PIC exhibits also two steps decomposition process, the first degradation ranges from 308 °C to 383 °C with a mass loss of 93.9% which is assigned to the depolymerization of PIC [37]. The second step was from 383 °C to 530 °C which is assigned to the formation and degradation of a transient char. PBS and PIC exhibit no residual char after the experiment.

When APP was incorporated into PBS, there are two steps of decomposition process. In the first step, incorporation of APP accelerates the beginning of the degradation, T2% is lowered by 26 °C in comparison to neat PBS. The first step has 72% of mass loss which can be assigned to the decomposition of the APP and the depolymerization of PBS. The second step was between 350 °C and 570 °C and is assigned to the formation and the degradation of transient char. It should be mentioned that after 570 °C, the residual char of PBS/APP was not stable, and the mass of the residue continuously decreases from 12.8% at 570 °C to only 3.7% at 800 °C. When PIC is incorporated into PBS and APP, there are still two decomposition steps. The T2% (306 °C) is not modified compared to that of PBS/APP (309 °C). However, the mass loss of the first step is 78% which is 6% more than that obtained with PBS/APP. thus at the beginning of the second step, the residual mass of PBS/PIC/APP is 6% lower than that of PBS/APP. This result shows that the char yield of PBS/APP is higher than that of PBS/PIC/APP during the formation of char. The curve of PBS/PIC/APP formed a steady plateau with 8.9% of residue from 600 °C to 800 °C. To understand the role of PIC in the intumescent formulation, PIC/APP with a ratio of 1/3 was also investigated. PIC/APP exhibits also two decomposition steps. The first step starts from 286 °C (T2%) to 350 °C with only 31% of mass loss. Then the second steps was from 350 °C to 600 °C with 41% of mass loss which can be assigned to the formation and degradation of transient char. The residual mass reaches 12.5%.

Differential TG curves (which is the result of the difference between the experimental TG curve and the calculated one) were plotted for PBS/APP, PIC/APP and PBS/PIC/APP. This permits to investigate potential interactions between PBS, PIC and APP (Fig. 9). PBS/APP exhibits a significant destabilization between 320 and 420 °C. This strong destabilization indicates that APP promotes the decomposition of PBS. PIC/APP exhibits also a destabilization at this range of temperature but which is less intense. A second destabilization was observed from 500 °C to 600 °C for PIC/APP formulation, which can be assigned to the degradation of the transient char. In the case of PBS/PIC/APP and PBS/APP this destabilization is smaller.

To investigate the decomposition behavior of PBS/APP and PBS/PIC/APP during the MLC test, additional TGA tests with special heating rate were analyzed (Fig. 10 a). For PBS/APP, starting from 30 °C to 305 °C (162 °C/min) then 31 °C/min until 490 °C followed by an isotherm for a total time of 800s. For PBS/PIC/APP, starting from 30 °C to 295 °C (165 °C/min) then 22 °C/min until 370 °C followed by an isotherm for a total time of 600s.

During the first step of heating, PBS/APP and PBS/PIC/APP had no significant mass loss. During the second step of heating, the mass loss for PBS/APP began at 2.71min around 338 °C, and the major mass loss was between 3.58 min and 4.88 min around 383 °C, 78% of mass loss was obtained, a plateau was observed. As for PBS/PIC/APP, the mass loss began at 2.73 min around 323 °C, and the major mass loss was between 4.45 min and 4.75 min round 365 °C, only 15% of mass loss was obtained. During the third step, a great mass loss for PBS/PIC/APP was observed until a plateau appeared at 370 °C. Both PBS/APP and PBS/PIC/APP had about 20% of residue, which can be assigned to the formation of the char corresponding to the same phenomenon in Fig. 8. It must be mentioned that when APP had the same experiment condition as PBS/APP or PBS/PIC/APP, its decomposition process can be assigned to the release of water and ammonia as well as the formation of P-O-P structure (Fig. 10 b). APP's decomposition with the experiment condition of PBS/PIC/APP was slower than that of PBS/APP, which reveals that the released gases should have been less. Obviously, these results evidenced that PBS/PIC/APP decomposes slower than PBS/APP, which can be a reason why in MLC test, the mass loss rate of PBS/PIC/APP was slower than that of PBS/APP, and that the HRR of PBS/PIC/APP was always lower than that of PBS/APP.

3.5. Investigation of char morphology

The morphology of the char is investigated at multi-scale using optical microscopy (mm scale) and scanning electron microscopy (SEM) (μm scale), then by using electron probe micro analysis (EPMA) (chemical composition at μm scale), the distribution of the phosphorus which can be involved in the mechanism of action is presented.

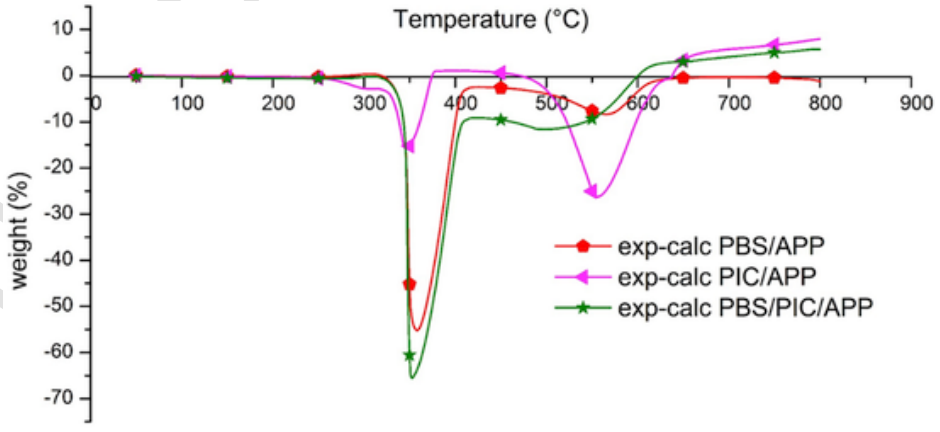

Fig. 9. Differential TGA of PBS/APP, PIC/APP and PBS/PIC/APP under thermo-oxidative condition (10 °C/min, Air).

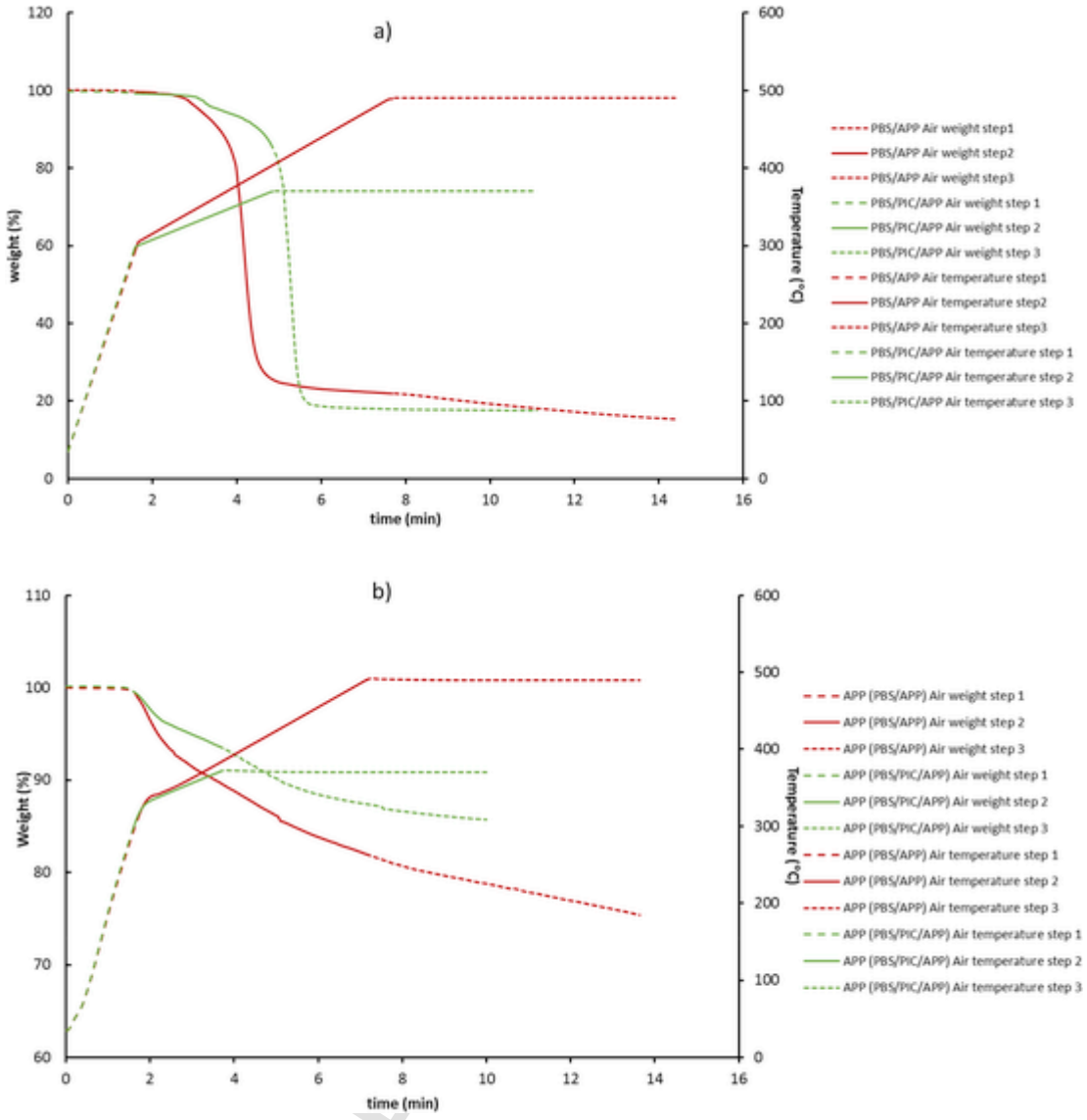

Fig. 10. TGA of a) PBS/APP, PBS/PIC/APP and b) APP with the same heating condition of MLC test.

3.5.1. Char morphology investigated by optical microscope

The char residues of PBS/APP and PBS/PIC/APP were collected and cut on the side face. The flank side of out layer of the char is presented in Fig. 11 a) for PBS/APP and Fig. 11 b) for PBS/PIC/APP. The layer of the char of PBS/APP has 2.8–3.5 mm of thickness, whereas the layer of the char of PBS/PIC/APP has only 1.0–1.4 mm of thickness. The outside of the char showed no significant difference between these two formulations (not presented) on optical microscope. Then the inner side of these two chars layer are presented in Fig. 11 c) for PBS/APP and Fig. 11 d) for PBS/PIC/APP. The inner side of PBS/APP is porous with numerous holes of different sizes. However, PBS/APP/PIC has smaller and less holes on inner side of its char. The obvious differences of the chars between these two formulations may explain the different performance in the MLC test. Indeed, according to mass loss and temperature measured during the MLC test Fig. 4 b) Fig. 4 c), PBS/PIC/APP showed lower temperature under the char and less mass loss rate (the mass loss rate between 250 s and 500 s decreased from 0.17%/s for PBS/APP to 0.13%/s for PBS/PIC/APP), which released less degradation products during the combustion, thus it has less and smaller holes on the inner side of the char.

3.5.2. Char morphology investigated by SEM and EPMA

Although the outside of the char layers showed no significant difference between PBS/APP and PBS/PIC/APP with optical microscope, they were also investigated at μm scale by SEM (Fig. 12). On the exterior side, the surface of the char layer of PBS/PIC/APP is homogenous and no significant defect can be distinguished. Whereas, the surface of the char of PBS/APP has cracks and small holes.

At the same time of analysis of SEM, the phosphorus distribution is measured by EPMA. As presented in Fig. 11, the outside of the char layer [A out) PBS/APP and B out) PBS/PIC/APP] and inner side of the char layer [A in) PBS/APP and B in) PBS/PIC/APP] were analyzed. The exterior side of the char of PBS/PIC/APP shows that the phosphorus is mainly located on a very thin layer Fig. 13 B out), which is 50–150 μm thick in size. Despite the low thickness of this layer, there is almost no defect and the phosphorus is highly concentrated on this thin layer. In the case of PBS/APP, on the exterior char, the distribution of phosphorus is on a thick layer of 500–1000 μm Fig. 13 A out). The distribution of the phosphorus is not homogenous and zone without P in this layer can be distinguished. Note that the concentration of the phosphorus is lower than that found in the case of PBS/PIC/APP. The inner side of

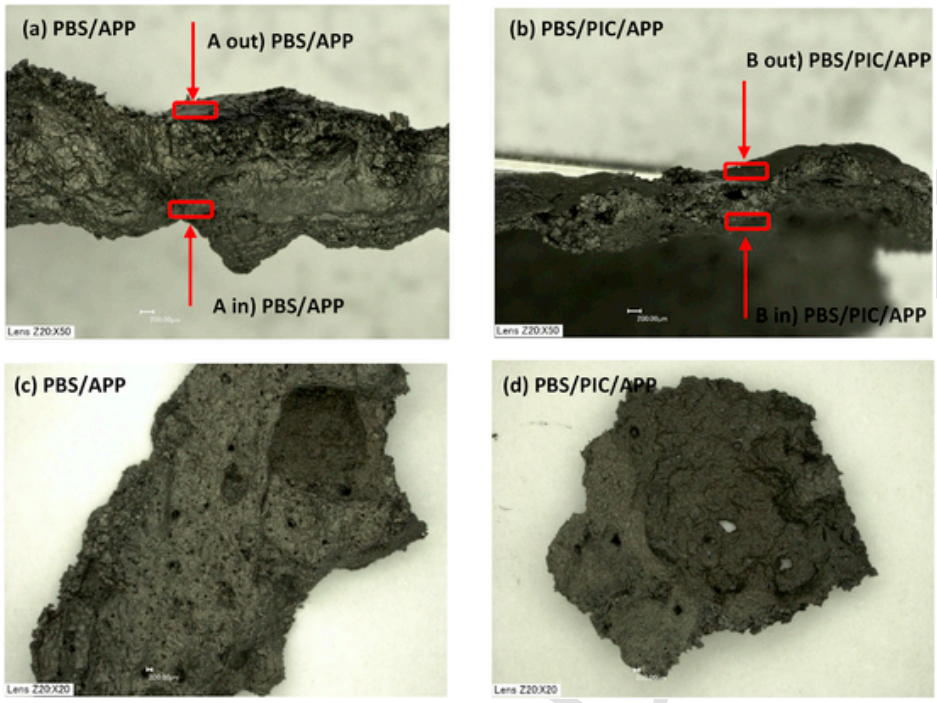

Fig. 11. Observation of the residual char by optical microscope: a) flank of residual char layer of PBS/APP, b) flank of residual char layer of PBS/PIC/APP, c) inner surface of the char layer of PBS/APP, d) inner surface of the char layer of PBS/PIC/APP.

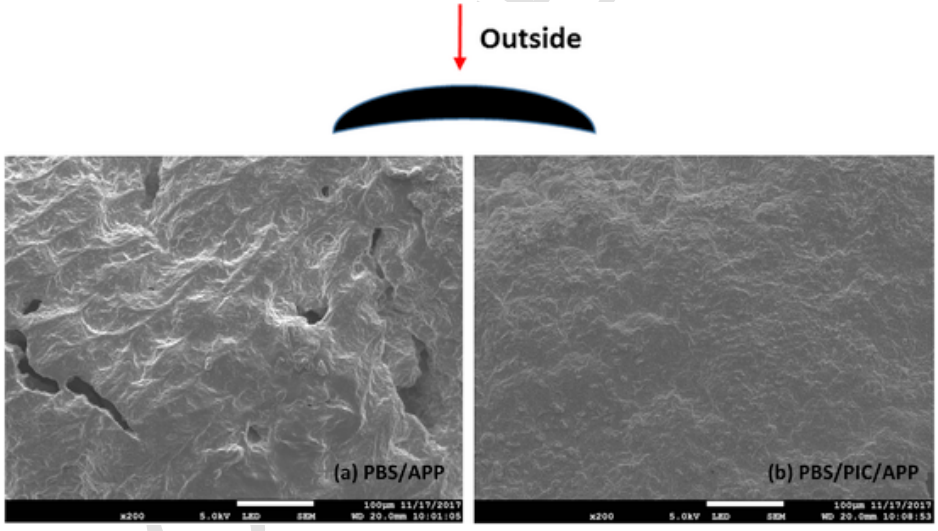

Fig. 12. Observation of the residual char by SEM: a) surface of residual char of PBS/APP, b) surface of residual char of PBS/PIC/APP.

the char shows different behaviors for the two formulations as well. For PBS/PIC/APP, the distribution of the phosphorus shows the presence of cavity of different size Fig. 13 B in). A mechanism of the formation of this cavity can be proposed: i) combustible gases were released during the decomposition of the polymer, and these gases diffuse to the surface of the char; ii) inner side of the char has a low temperature, thus the amount of degradation products (released gases) were much less than that of PBS/APP; iii) the char layer of PBS/PIC/APP which had some permeability cannot perfectly isolate these gases from the flame, however it keeps still an internal pressure which reduce the diffusion speed of the combustible gases, and it can be confirmed by the mass loss curve (PBS/PIC/APP has lower mass loss rate than PBS/APP); iv) thus the char of PBS/PIC/APP may have a lower permeability than PBS/APP and the combustible gases have a lower diffusion speed, hence the combustible gases formed cavity structure instead of creating 'tunnel' like passage in the char. Moreover, the concentration of the phosphorus is relatively low compared to the distribution of phosphorus on the exterior char, which reveals that phosphorus in the char is concentrated at the surface. In the case of PBS/APP, on the inner side of the char shows no cavity structure (tunnel like structure), and the concentration of the phosphorus is higher than that obtained in PBS/PIC/APP Fig. 13 A in).

In conclusion, significant differences of the P distribution of the inner side and exterior side of the char layer can explain why smaller and less holes were observed on the surface of PBS/PIC/APP. Furthermore, the cavity structure in PBS/PIC/APP reveals that the combustible gases were trapped in the char, and that indicates a slower diffusion of the combustible gases in the char which can reduce the supply of 'fuel' in MLC test, thus lower pHRR and THR were obtained in the case of PBS/PIC/APP.

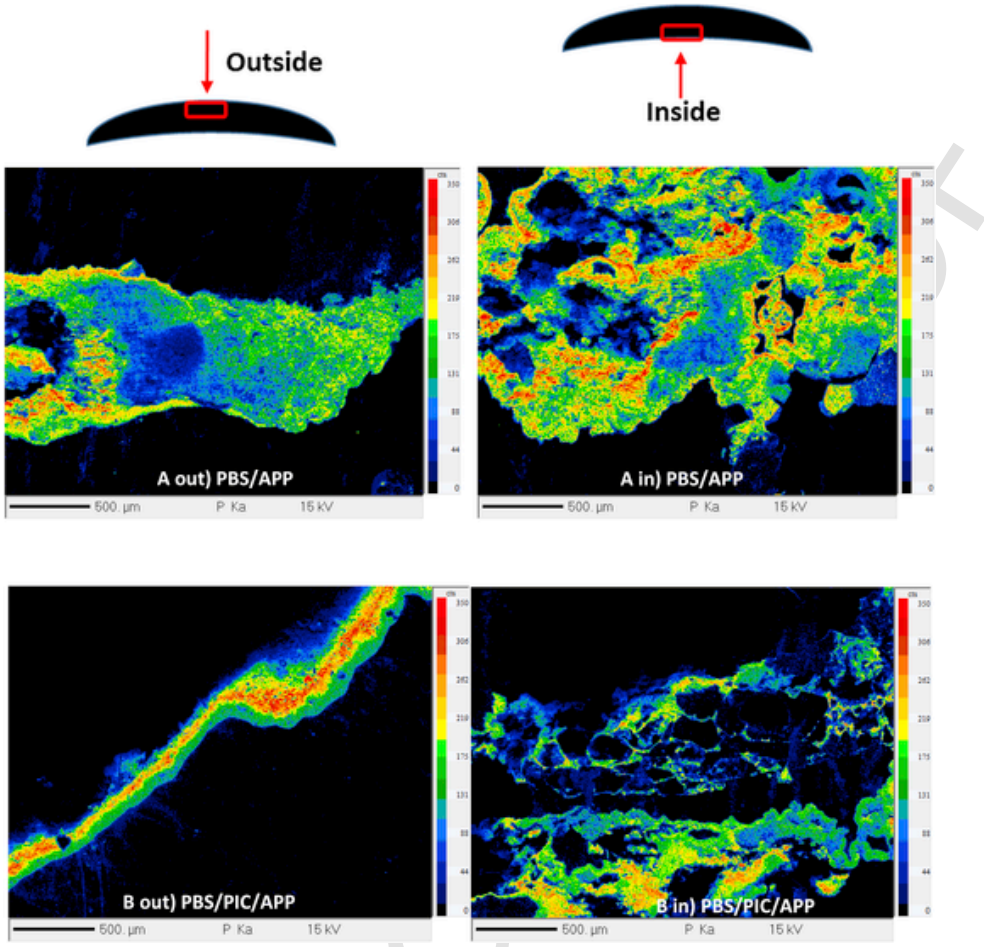

Fig. 13. Phosphorus distribution of the residual char on the flank side: A out) out side of the char layer of PBS/APP, B out) out side of the char layer of PBS/PIC/APP, A in) inner side of the char layer of PBS/APP, B in) inner side of the char layer of PBS/PIC/APP.

3.6. Proposed mode of action in MLC test

With the evidences provided above, the mechanism of PBS/PIC/APP was determined (Fig. 14). At the beginning of the test (before 100 s), PBS and PIC starts to melt and decompose releasing combustible gases (majorly THF and succinic anhydride) [38]. Meanwhile, APP decompose and release H_2O and NH_3. Then PBS/APP and PBS/PIC/APP start to burn at almost the same time (100 s). Between 100 s and 450 s, intumescent char which is mainly consisted of orthophosphates, pyrophosphate, aliphatic and aromatic groups are formed. The char of PBS/PIC/APP showed a glass-type structure, and the phosphates concentrate on the surface of the char layer leading to a more resistant barrier to heat, and it leads to lower mass loss rate, heat release rate than PBS/APP. After the combustion, cavity structure was found in the char of PBS/PIC/APP, whereas 'tunnel' type structure was found in the char of PBS/APP, which indicate a lower diffusion speed of the combustible gases presented in the char of PBS/PIC/APP. Therefore, PBS/PIC/APP has lower THR and pHRR than PBS/APP.

4. Conclusion

It was showed that during the MLC test, the intumescent char formed by PBS/PIC/APP has better heating-rate-decreasing effect than that of PBS/APP. A glass type char with phosphorus concentrated on the surface in PBS/PIC/APP governed its performance: this char showed lower gases diffusion speed leading to lower mass loss rate. This study demonstrated that addition of only 7.5 *wt*% of PIC in PBS/APP can improve significantly the flame retardancy of this intumescent FR system. It evidences that isosorbide-based compounds can act as carbonization agent in an intumescent FR system. Besides the improvement of flame retardancy, the application of PIC improves the ratio of bio-based components, the double benefits lead to more ideas of using the bio-based components to flame retard polymeric materials.

CRediT authorship contribution statement

Chi Hu: Conceptualization, Investigation, Writing - original draft. **Serge Bourbigot:** Conceptualization, Validation, Writing - review & editing, Supervision. **Thierry Delaunay:** Project administration, Funding acquisition. **Marion Collinet:** Project administration, Funding acquisition. **Sophie Marcille:** Resources, Funding acquisition. **Gaëlle Fontaine:** Conceptualization, Validation, Writing - review & editing, Supervision.

Acknowledgment

The authors thank Bertrand Revel and Bertrand Doumert of plateforme RMN of université de Lille for their help to accomplish the solid state NMR analysis and Séverine Bellayer for her help to achieve the SEM, EPMA and optical microscope.

This study was financially supported by Institut Français des Materiaux Agro-Sourcés (France), Program Investissement d'Avenir (France) and Roquette Frère (France)

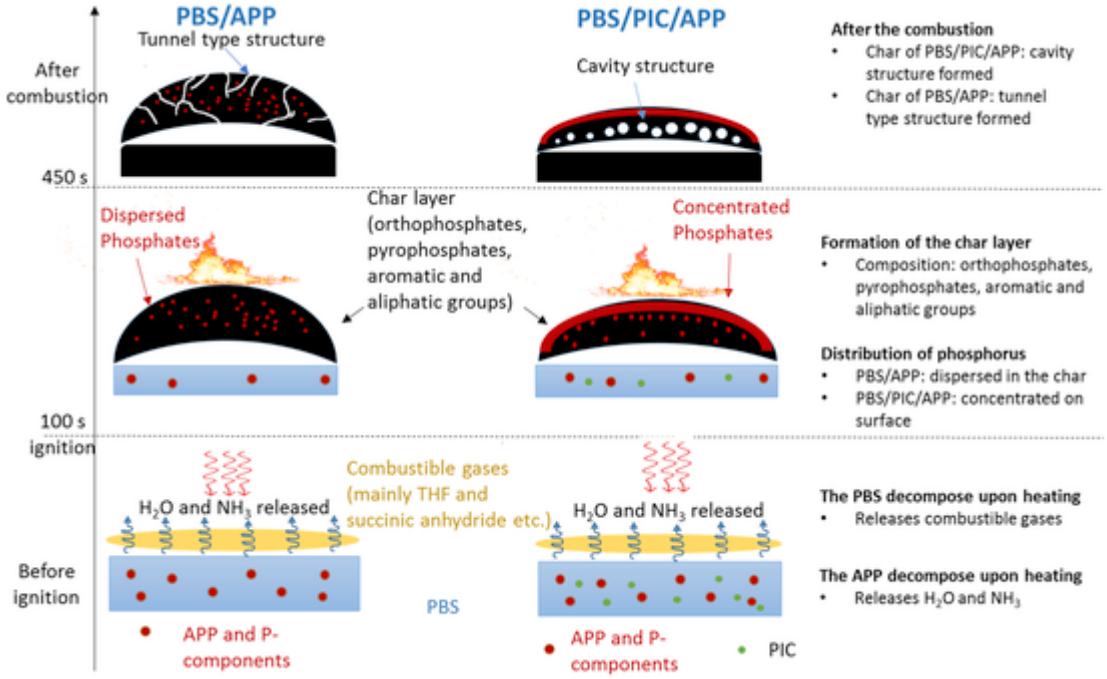

Fig. 14. Proposed mechanism of PBS/PIC/APP and PBS/APP.

Appendix A. Supplementary data

Supplementary data to this article can be found online at https://doi.org/10.1016/j.compositesb.2019.107675.

References

[1] T Fujimaki. Processability and properties of aliphatic polyesters,'BIONOLLE', synthesized by polycondensation reaction. Polym Degrad Stab 1998;59(1–3):209–214.

[2] J Zeng, L Jiao, YD Li, M Srinivasan, T Li, YZ Wang. Bio-based blends of starch and poly(butylene succinate) with improved miscibility, mechanical properties, and reduced water absorption. Carbohydr Polym 2011;83(2):762–768.

[3] T Ohkita, SH Lee. Crystallization behavior of poly(butylene succinate)/corn starch biodegradable composite. J Appl Polym Sci 2005;97(3):1107–1114.

[4] N Lin, DK Fan, PR Chang, JH Yu, XC Cheng, J Huang. Structure and properties of poly(butylene succinate) filled with lignin: a case of lignosulfonate. J Appl Polym Sci 2011;121(3):1717–1724.

[5] S Nie, X Liu, G Dai, S Yuan, F Cai, B Li, et al. Investigation on flame retardancy and thermal degradation of flame retardant poly(butylene succinate)/bamboo fiber biocomposites. J Appl Polym Sci 2012;125(S2):485–489.

[6] L Liu, G Huang, P Song, Y Yu, S Fu. Converting industrial alkali lignin to biobased functional additives for improving fire behavior and smoke suppression of polybutylene succinate. ACS Sustainable Chem Eng 2016;4(9):4732–4742.

[7] H Chen, T Wang, Y Wen, X Wen, D Gao, R Yu, et al. Expanded graphite assistant construction of gradient-structured char layer in PBS/$Mg(OH)_2$ composites for improving flame retardancy, thermal stability and mechanical properties. Compos B Eng 2019;177:107402–107410.

[8] CF Kuan, HC Kuan, CCM Ma, CH Chen. Flame retardancy and non dripping properties of ammonium polyphosphate/poly(butylene succinate) composites enhanced by water crosslinking. J Appl Polym Sci 2006;102(3):2935–2945.

[9] Y Chen, J Zhan, P Zhang, S Nie, H Lu, L Song, et al. Preparation of intumescent flame retardant poly(butylene succinate) using fumed silica as synergistic agent. Ind Eng Chem Res 2010;49(17):8200–8208.

[10] YJ Liu, L Mao, SH Fan. Preparation and study of intumescent flame retardant poly(butylene succinate) using MgAlZnFe-CO3 layered double hydroxide as a synergistic agent. J Appl Polym Sci 2014;131(17):40736–40745.

[11] HY Yang, L Song, QL Tai, X Wang, B Yu, Y Yuan, et al. Comparative study on the flame retarded efficiency of melamine phosphate, melamine phosphite and melamine hypophosphite on poly(butylene succinate) composites. Polym Degrad Stab 2014;105:248–256.

[12] X Wang, L Song, HY Yang, HD Lu, Y Hu. Synergistic effect of graphene on antidripping and fire resistance of intumescent flame retardant poly(butylene succinate) composites. Ind Eng Chem Res 2011;50(9):5376–5383.

[13] X Wang, Y Hua, L Song, HY Yang, B Yua, B Kandola, et al. Comparative study on the synergistic effect of POSS and graphene with melamine phosphate on the flame retardancy of poly(butylene succinate). Thermochim Acta 2012;543:156–164.

[14] S Bourbigot, M Le Bras, F Dabrowski, JW Gilman, T Kashiwagi. PA-6 clay nanocomposite hybrid as char forming agent in intumescent formulations. Fire Mater 2000;24(4):201–208.

[15] M Bugajny, M Le Bras, S Bourbigot. New approach to the dynamic properties of an intumescent material. Fire Mater 1999;23(1):49–51.

[16] M Le Bras, M Bugajny, JM Lefebvre, S Bourbigot. Use of polyurethanes as char-forming agents in polypropylene intumescent formulations. Polym Int 2000;49(10):1115–1124.

[17] M Bugajny, M Le Bras, S Bourbigot, R Delobel. Thermal behaviour of ethylene-propylene rubber/polyurethane/ammonium polyphosphate intumescent formulations —a kinetic study. Polym Degrad Stab 1999;64(1):157–163.

[18] M Le Bras, S Bourbigot, Y Le Tallec, J Laureyns. Synergy in intumescence—application to β-cyclodextrin carbonisation agent in intumescent additives for fire retardant polyethylene formulations. Polym Degrad Stab 1997;56(1):11–21.

[19] M Le Bras, S Bourbigot, C Delporte. New intumescent formulations of fire-retardant polypropylene-discussion of the free radical mechanism of The formation of carbonaceous protective material during the thermo-oxidative treatment of the additives. Fire Mater 1996;20(4):191–203.

[20] JR Van Wazer, CF Callis, JN Shoolery, RC Jones. Principles of phosphorus chemistry. II. Nuclear magnetic resonance measurements. J Am Chem Soc 1956;78(22):5715–5726.

[21] TM Duncan, DC Douglass. On the phosphorus-31 chemical shift anisotropy in condensed phosphates. Chem Phys 1984;87(3):339–349.

[22] IV Kovalev, NO Kovaleva. Organophosphates in agrogray soils with periodic water logging according to the data of 31P NMR spectroscopy. Eurasian Soil Sci 2011;44(1):29–37.

[23] MI Makarov, L Haumaier, W Zech. The nature and origins of diester phosphates in soils: a 31P-NMR study. Biol Fertil Soils 2002;35(2):136–146.

[24] S Bourbigot, M Le Bras, R Delobel, R Decressain, J Amoureux. Synergistic effect of zeolite in an intumescence process: study of the carbonaceous structures using solid-state NMR. J Chem Soc, Faraday Trans 1996;92(1):149.

[25] G Walter, U Hoppe, J Vogel, G Carl, P Hartmann. The structure of zinc polyphosphate glass studied by diffraction methods and 31P NMR. J Non-Crist Solids 2004;333(3):252–262.

[26] WJ Kroenke. Low-melting sulphate glasses and glass-ceramics, and their utility as fire and smoke retarder additives for poly(vinyl chloride). J Mater Sci 1986;21(4):1123–1133.

[27] C Ciulik, M Safari, AM Ilarduyaa, JC Morales-Huerta, A Iturrospe, A Arbe, et al. Poly(butylene succinate-ran-ε-caprolactone) copolyesters: enzymatic synthesis and crystalline isodimorphic character. Eur Polym J 2017;95:795–808.

[28] T Dong, Y He, K Shin, Y Inoue. formation and characterization of inclusion complexes of poly(butylene succinate) with a- and g-cyclodextrins. Macromol Biosci 2004;4(12):1084–1091.

[29] Q Li, WX Zhu, CC Li, GH Guan, D Zhang, YN Xiao, et al. A non-phosgene process to homopolycarbonate and copolycarbonates of isosorbide using dimethyl carbonate: synthesis, characterization, and properties. J Polym Sci, Polym Chem Ed 2013;51(6):1387–1397.
[30] GE Maciel, VJ Bartuska, FP Miknis. Characterization of organic material in coal by proton-decoupled ^{13}C nuclear magnetic resonance with magic-angle spinning. Fuel 1979;58(5):391–394.
[31] G Camino, L Costa, G Clouet, A Chiotis, J Brossas, M Bert, et al. Thermal degradation of phosphonated polystyrenes: Part 1—chain end condensation. Polym Degrad Stab 1984;6(2):105–121.
[32] GE Maciel, MJ Sullivan, L Petrakis, DW Grandy. ^{13}C Nuclear magnetic resonance characterization of coal macerals by magic angle spinning. Fuel 1982;61(5):411–414.
[33] G Camino, L Costa, L Trossarelli. Study of the mechanism of intumescence in fire retardant polymers: Part V--Mechanism of formation of gaseous products in the thermal degradation of ammonium polyphosphate. Polym Degrad Stab 1985;12(3):203–211.
[34] G Camino, MP Luda. Mechanistic study on intumescence. In: M Le Bras, G Camino, S Bourbigot, R Delobel, editors. Fire retardancy of polymers, the use of intumescence. Cambridge: The Royal Society of Chemistry; 1998. p. 48–63.
[35] HL Vandersall. Intumescent coating systems, their development and chemistry. Journal of Fire and Flammability 1971;2:97–140.
[36] K Chrissafis, KM Paraskevopoulos, DN Bikiaris. Thermal degradation mechanism of poly(ethylene succinate) and poly(butylene succinate): comparative study. Thermochim Acta 2005;435(2):142–150.
[37] JH Park, MS Koo, SH Cho, MY Lyu. Comparison of thermal and optical properties and flowability of fossil-based and bio-based polycarbonate. Macromol Res 2017;25(11):1135–1144.
[38] YF Shih. Thermal degradation and kinetic analysis of biodegradable PBS/multi-walled carbon nanotube nanocomposites. J Polym Sci, Polym Phys Ed 2009;47(13):1231–1239.